**Annales
Geophysicae**

Statistical characteristics of low-latitude ionospheric field-aligned irregularities obtained with the Piura VHF radar

J. L. Chau[1,2]**, R. F. Woodman**[1]**, and L. A. Flores**[2]

[1]Radio Observatorio de Jicamarca, Instituto Geofísico del Perú, Lima, Perú
[2]Laboratorio de Física, Universidad de Piura, Piura, Perú

Abstract. We present a summary of the statistical characteristics of echoes from ionospheric (E- and F-region) field-aligned irregularities obtained with the Piura VHF radar. This radar is located at $\sim 7.0°$ dip latitude, just outside the equatorial electrojet (EEJ) region. Our results are based on (1) intermittent observations made between 1991 and 1999 just few days a year, and (2) continuous observations made between January 2000 and June 2001. During most of the intermittent observations, simultaneous measurements of EEJ and equatorial spread F (ESF) irregularities were performed with the Jicamarca VHF radar. From the continuous measurements, we have obtained the diurnal and seasonal characteristics of a variety of parameters (percentage of occurrence, signal-to-noise ratio and/or Doppler velocities) from the lower and upper E-region irregularities and also from F-region irregularities over Piura. For example, we have found that (1) the E-region echoes are stronger and occur more frequently during local summer (i.e. between December and March); (2) between May and June, the E-region echoes are weaker and occur less frequently; moreover, during these months, a semidiurnal wave with large amplitudes is observed in the meridional wind ($> 100\,\mathrm{m\,s^{-1}}$); (3) there is vertical wavelength of about 20 km in the Doppler velocity, particularly after midnight; (4) the lower (upper) E-region Doppler velocities are influenced mainly by meridional winds (equatorial F-region vertical drifts). In addition, we have observed that the seasonal and daily occurrences of Piura F-region irregularities are similar to the occurrence of topside ESF irregularities over Jicamarca. The likelihood of occurrence of F-region irregularities over Piura and, therefore, topside ESF over Jicamarca is greater when there are no E-region irregularities over Piura. On the other hand, there is more probability of observing bottomtype/bottomside ESF irregularities over Jicamarca when E-region irregularities are observed over Piura.

Key words. Ionosphere (ionospheric irregularities; equatorial ionosphere; instruments and techniques)

---

1 Introduction

At low latitudes, but outside the equatorial electrojet (EEJ) region, i.e. $\pm 3°$ off the dip equator (e.g. Forbush and Casaverde, 1961), the characteristics of the ionospheric irregularities are not well known, mainly because there have been only few observational and theoretical studies at these latitudes. On the other hand, ionospheric field-aligned irregularities (FAI) have been intensively studied in the equatorial and auroral regions with radars and in situ measurements (see, e.g. Kelley, 1989). In the last decade, intensive efforts (radar, optical and in situ observations, modeling) have been dedicated to the understanding of FAI at mid-latitudes (e.g. Fukao et al., 1998; Larsen, 2000 and references therein for E-region studies; and Fukao et al., 1991, Swartz et al., 2000 for F-region studies). Special emphasis has been placed on the understanding of the so-called "quasi-periodic" (QP) echoes first observed by Yamamoto et al. (1991) (see, e.g. Hysell and Burcham, 2000 and references therein).

The few radar observations at low latitudes have been made with the Indian VHF radar in Gadanki (13.5° N, 79.2° E; dip latitude 12.5° N) (e.g. Choudhary et al., 1996; Krishna Murthy et al., 1998; Choudhary and Mahajan, 1999; Patra et al., 1997; Rao et al., 1997), the Piura VHF radar in Peru (5.2° S, 80.63° W; dip latitude 13.9° N) (Woodman et al., 1999; Chau and Woodman, 1999) and with a forward-scatter radar system installed in South America during the International Geophysical Year (IGY) (Cohen and Bowles, 1963).

The main characteristics of the E-region echoes at these low latitudes are very similar to those observed at mid-latitudes, i.e. they occur mainly at night, are produced by gradient drift instabilities, where the lower echoes are of a continuous type and the upper E-region echoes are of QP type. On the other hand, the few F-region observations present very similar characteristics to the equatorial F-region irreg-
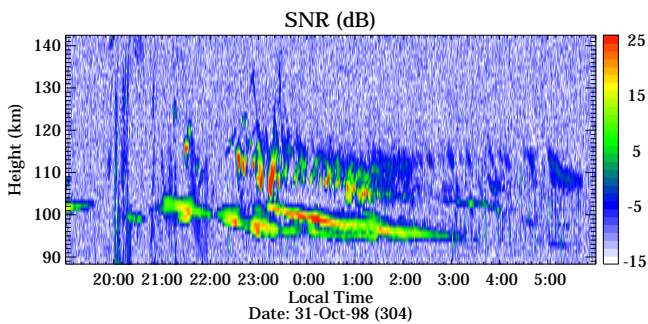
SNR (dB)

Fig. 1. Example of altitude-time signal-to-noise ratios from E-region irregularities.

ularities, particularly those from the topside (e.g. Patra et al., 1997).

In addition to the scientific importance of understanding the morphology of ionospheric FAI at these latitudes, there is the need to study the possible relationship between FAI at these latitudes and the occurrence of ESF irregularities at the dip equator, since F-region magnetic flux tubes over the dip equator map into the E-region heights at low latitudes. This relationship could help with the forecasting of the ESF irregularities.

The Piura VHF radar constitutes the easternmost element of a network of atmospheric radars located close to the geographic equator in the Pacific Ocean sector (see Gage et al., 1991 for details on these radars). The main purpose of this radar is to study the lower atmospheric dynamics operating as a wind profiler. Between 1991 and 1999, we have sporadically interrupted its normal observations to study the characteristics of E-region and F-region irregularities. Preliminary results have been published by Woodman et al. (1999) and Chau and Woodman (1999). Although the Piura observations are taken at a similar magnetic latitude as the Gandaki radar in India, they are very unique, since Piura is located in the southern geographic hemisphere.

In this paper, we extend the results presented by Woodman et al. (1999) based on 15 days of data, by making use of more data taken intermittently between 1991 and 1999. Particular emphasis is given to the concurrent observations of FAIs between the Piura and the Jicamarca radars. Then we present and discuss the statistical characteristics (diurnal and seasonal) obtained from new data taken between January 2000 and June 2001. During this period, ionospheric observations have been made on a "continuous" fashion without interrupting the lower atmospheric observations, but with a poorer time resolution compared to the previous observations (see details below).

2 Results from intermittent observations

In this section, we present the results obtained between 1991 and 1999 from intermittent Piura campaigns dedicated exclusively to the observations of E- and F-region irregulari-

ties. Coincidentally, one of the predefined pointing directions of the Piura VHF radar, points perpendicular to the magnetic field, i.e. ~14° zenith angle to the north; therefore, we needed only to modify the acquisition parameters to perform these experiments.

The basic parameters of the Piura radar are the 49.920-MHz operating frequency, an 100 m × 100 m antenna area, ~2.1° two-way half-power beam width, and 20 kW of transmitted peak power. More details on this system are given by Gage et al. (1991).

2.1 Intermittent E-region observations

The main features of E-region irregularities obtained from these intermittent campaigns have already been presented by Woodman et al. (1999) and Chau and Woodman (1999). Here we present just one example and summarize the results previously obtained in order to avoid duplication. In Fig. 1, we show altitude-time signal-to-noise ratio (SNR) values obtained from E-region irregularities observed on 31 October 1998. In this particular example we are able to clearly distinguish between the two regions described by Woodman et al. (1999), namely the lower, continuous-type E-region echoes $(95 - 105\,\text{km})$ and the upper, patchy-type E-region echoes $(105 - 120\,\text{km})$. As it can be seen, the latter echoes, when observed with high time resolution, show quasi-periodic characteristics like those reported at mid-latitudes. The co-existence of echoes from both regions has also been shown by Choudhary and Mahajan (1999).

The main characteristics of these E-region echoes are:

– They appear mainly at night, between 19:00 LT and 06:00 LT. Their spectral widths range from 30 to $100\,\text{m s}^{-1}$ and their mean Doppler velocities vary between -30 and $30\,\text{m s}^{-1}$. The ratio of the spectral width to the mean Doppler velocity is greater than 1, implying that the echoes are due to gradient drift instabilities, i.e. type 2 echoes (e.g. Fejer and Kelley, 1980). Therefore, these low-latitude echoes resemble more the mid-latitude irregularities than the equatorial irregularities (e.g. Yamamoto et al., 1992; Haldoupis and Schlegel, 1996).

– There are two distinctive regions: one between 95 and 105 km and the other between 105 and 120 km. The lower region is less turbulent (mean spectral width of $\sim 60\,\text{m s}^{-1}$) than the upper region $(>75\,\text{m s}^{-1})$. In addition, the lower region echoes present a close-to-zero mean Doppler velocity, while the upper region echoes show a consistent positive velocity (downward/southward) $(7\,\text{m s}^{-1})$ (see also Patra and Rao, 1999).

– The upper region echoes present quasi-periodic echoes with negative and positive slopes (Chau and Woodman, 1999).

It is important to mention that although we have previously labeled the lower E-region echoes as "continuous", some-
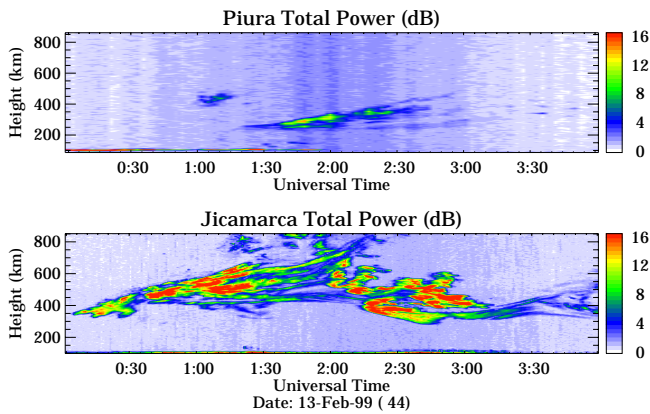
Fig. 2. Example of simultaneous power measurements of F-region field-aligned irregularities with the Piura (top) and Jicamarca (bottom) VHF radars.
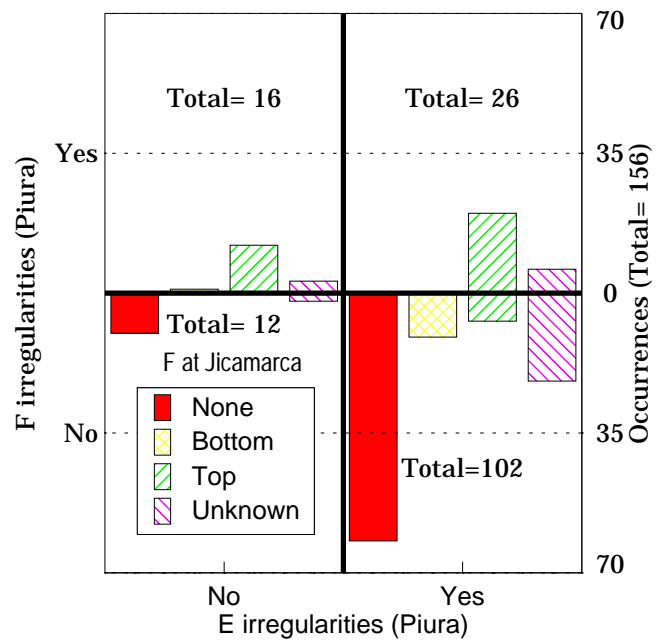

Fig. 3. Occurrence correlation between E and F-region irregularities observed over Piura and F-region irregularities observed over Jicamarca. These statistics have been obtained from 152 events obtained between 1991 and 1999. The different types of spread *F* events over Jicamarca are denoted with different patterns.

times structured echoes are observed, which are apparently very similar to those described by Urbina et al. (2000).

In addition, in Fig. 1, we can observe the presence of F-region echoes folding over our sampling window, around 20:15 LT. Note the striated characteristic of these echoes, starting at very low heights and covering almost all heights. In the next sections, we will discuss more about this "interference" and how we use it to obtain proxy measurements of F-region irregularities.

2.2 Intermittent F-region observations

As it has been mentioned before, on some occasions, simultaneous measurements were performed at Jicamarca, and were made with the JULIA system (these may be viewed from http://jro.igp.gob.pe/julia).

In Fig. 2, we present an example of simultaneous spread *F* measurements obtained with the Piura and the Jicamarca VHF radars. The Piura spread *F* echoes are weaker than the echoes from Jicamarca. Note that the Piura system has less sensitivity than Jicamarca (antenna size difference of −13 dB, transmitted power difference of −3 dB, and pulse width difference of −3 dB). There is a time difference of ∼16 min due to the difference in longitude, but that has been corrected in Fig. 2. So far, we have been able to observe only topside echoes (plume-type). There is a slight increase in the noise level in both sites around 02:00 LT (LT = UT - 5 h); this is due to the noise temperature at the center of the Galaxy.

Although the Piura spread *F* echoes are weaker than Jicamarca's, we have been able to use them to quantify the relationship between the occurrence of E- and F-region irregularities over Piura and the occurrence of F-region irregularities over Jicamarca. It is important to point out that F-region magnetic flux tubes over Jicamarca map into E-region heights at low latitudes. For the case of Piura, magnetic flux tubes at 200- and 300-km altitude over Jicamarca map to ∼100- and ∼200-km altitudes over Piura, respectively. In addition, we have used the Jicamarca ionograms when the

radar was not working, to determine the occurrence of spread *F* over Jicamarca.

In Fig. 3, we summarize the relationship between the Piura and Jicamarca irregularities based on 152 events taken between 1991 and 1999. The *x* (*y*) axis corresponds to the occurrence of Piura E-region (F-region) echoes. For each combination, the type of Jicamarca F-region irregularities is quantified, i.e. none (if no irregularities were observed), bottom (bottomtype or bottomside), top (plumes), and unknown (no data were available from Jicamarca). For a description on the different types of equatorial F-region irregularities, see Woodman and La Hoz (1976) and Hysell and Burcham (1998).

The main results from this diagram are:

– E-region echoes are observed most of the time (lower right quarter).

– When F-region echoes are observed over Piura, plume-type echoes are observed over Jicamarca (first row).

– The likelihood of obtaining F-region irregularities at Piura and, therefore, topside ESF irregularities at Jicamarca is about half if there are no E-region irregularities, but only about one-fifth if there are E-region irregularities.

– There is more probability to observe bottom-type/bottomside ESF irregularities over Jicamarca when E-region irregularities are observed over Piura.
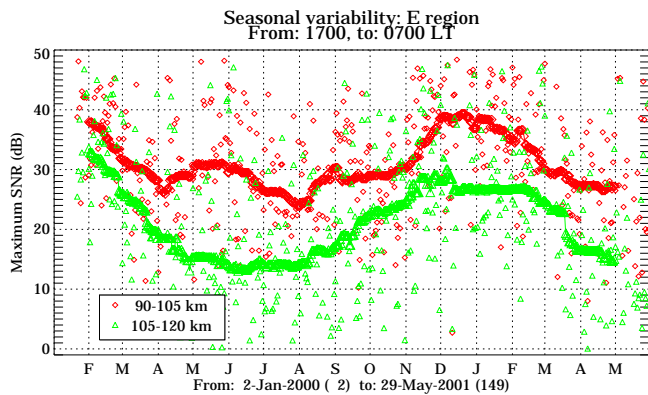
Fig. 4. Seasonal variability of maximum daily SNR observed from the lower E-region (red) and the upper E-region (green). The thicker symbols represent 60-day median averages.

3   Results from continuous observations

Since January 2000 we have been taking "continuous" measurements of E-region irregularities using the Piura VHF system. Every 12 min the system takes averaged spectra from the E-region ($85 - 140$ km) for about 1 min, with similar parameters to those used in the intermittent experiments (see Woodman et al., 1999 for details). During the other 11 min, the system works in its normal way, i.e. it cycles through different beam positions in order to obtain the three-dimensional wind vector of lower atmospheric heights. Therefore, this new E-region data set is not ideal for studies where good time resolution is needed (e.g. quasi-periodic echoes). Nonetheless, since these measurements are made unattended and continuous, as we show below, this data set allows us to obtain good statistical characteristics of these echoes.

3.1   Continuous E-region observations

In Fig. 4, we show the daily maximum SNR from January 2000 to June 2001. Again, we have obtained the statistics for the two regions mentioned above, lower (in red) and upper (in green). The thicker symbols represent 60-day median averages. Since the stronger echoes occur mainly at night, the maximum SNR is calculated just from nighttime hours. In both regions, the maximum SNRs occur from mid-November to mid-March (i.e. centered around the summer months). On the other hand, the weaker echoes (up to 15 dB less) tend to occur between May and August. In addition, there is a strong day-to-day variability in both regions.

The daily percentage of occurrence of E-region echoes shown in Fig. 5 represents the fraction of the time that E-region echoes were observed between 17:00 LT and 07:00 LT. We have used a threshold SNR value of -3 dB to decide if irregularities were observed or not. As in Fig. 4, statistics are obtained for both regions, and 60-day median averages have been estimated.
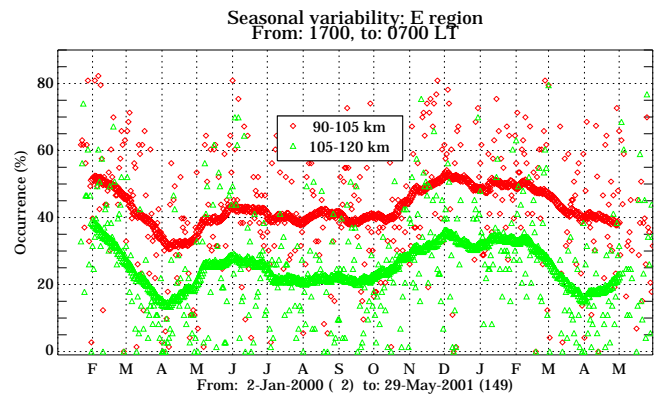

Fig. 5. Seasonal variability of percentage of occurrence of lower E-region (red) and the upper E-region (green) irregularities. The thicker symbols represent 60-day median averages.
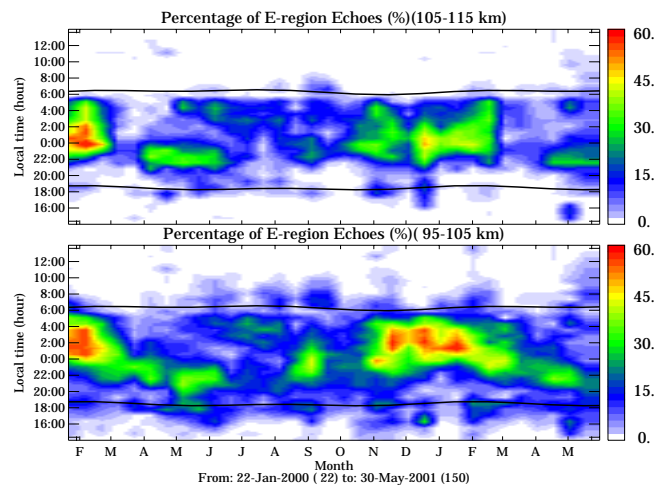

Fig. 6. Seasonal variability of the diurnal percentage of occurrence of lower E-region (bottom) and the upper E-region (top) irregularities. These statistics have been obtained by processing 15 days at the time. The local sunrise (sunset) times are shown with the upper (lower) black curve on each plot.

During the summer months, the daily percentage of occurrence is the highest ($\sim$50 % and $\sim$35 % for the lower and upper regions, respectively). As time moves away from (toward) the local summer months, the percentage of occurrence follows a (an) decrease (increase), with the lowest around mid-April. Although not shown here, on average, there is no significant dependence between the occurrence of nighttime low-latitude E-region echoes and geomagnetic activity.

Now we show in Fig. 6 the diurnal percentage of occurrence of E-region echoes as a function of the time of the year, again for the lower and upper regions. These values have been obtained by taking 15 days of data at the time (without repeating), and counting the number of good echoes (SNR > -3 dB) for every 45-min time interval.

The highest percentage occurs between 02:00 and 04:00 LT (23:00 and 01:00 LT) in the lower (upper) region
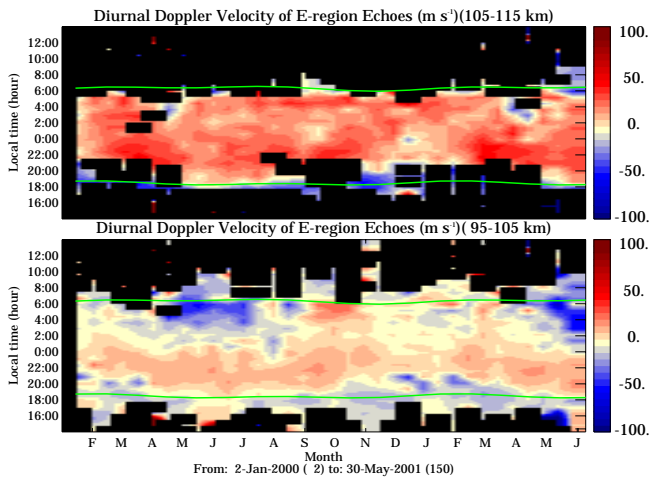
Fig. 7. Seasonal variability of the diurnal Doppler velocity from lower E-region (bottom) and the upper E-region (top) irregularities. These statistics have been obtained by processing 15 days at the time. The local sunrise (sunset) times are shown with the upper (lower) green curve on each plot.

during the summer months. Again, we can see that the echoes are observed during most of the nighttime of the summer months. The majority of the echoes disappear after 06:00 LT (right before local sunrise), particularly in the upper region, when photoionization in the E-region starts to increase.

From January to June, the lower echoes appear earlier as time increases (from 24:00 to 20:00 LT) in a narrow time interval (2 h), then suddenly the occurrence is shifted to the 03:00 to 06:00 time interval. Between April and June, the upper region echoes occur mainly between 21:00 and 24:00 LT.

In Fig. 7, the diurnal mean Doppler velocities (positive means towards the radar, i.e. downward/southward) are shown for the 18 months under study. We have only considered those values whose SNR is greater than −3 dB and the percentage of occurrence is greater than 2% (black color represents no valid data).

A clear annual periodicity is observed in the lower region, in addition to a semidiurnal pattern, particularly between April and July, where the mean Doppler velocities are positive between 19:00 and 24:00 LT and negative after midnight. The transition time from negative to positive velocities follows an annual periodicity, the latest occurred around 22:00 LT during the summer months, and the earliest occurred around 19:00 LT during the winter months. This pattern is similar to the local sunset time, although the time difference between the summer and the winter sunsets is not 3 h.

In the upper region there is also an annual periodicity, where the transition from negative to positive velocities is the earliest (19:00 LT) during the winter months, and is the latest during the summer months (22:00 LT). In this region, the Doppler velocities follow a diurnal pattern, contrary to the semidiurnal behavior observed in the lower region. In the
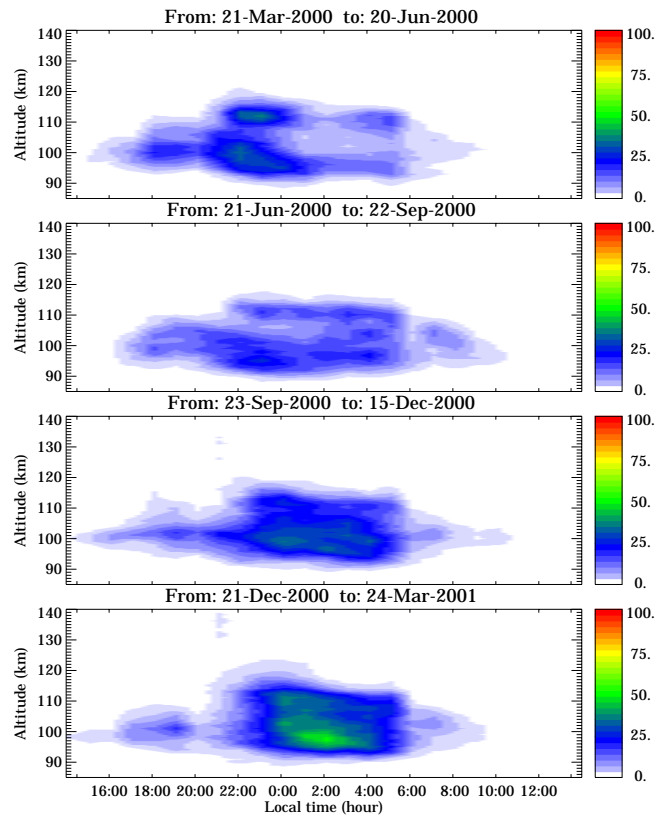

Fig. 8. Diurnal percentage of occurrence of E-region echoes as a function of altitude for different periods of the year: Fall, Winter, Spring, and Summer in the first, second, third and fourth rows, respectively.

few occasions where the velocities are negative, the percentage of occurrence and SNR (not shown) are very low.

Until now, in order to simplify the presentation of the results, we have presented them for two regions, i.e. lower and upper. In order to show that there is also important height-dependent information, in the next two figures we show the diurnal statistics (percentage of occurrence and mean Doppler velocity) as a function of altitude (every 1.0 km) for all four local seasons (fall, winter, spring and summer).

The percentage of occurrence presented in Fig. 8 shows a strong height dependence during the fall and winter seasons (first and second rows), where there are fewer echoes in between the lower and upper regions. Moreover, during these months there is a slightly larger occurrence of daytime echoes than during the other seasons. During the spring and summer seasons (third and fourth rows), there is no clear difference between the lower and upper regions. Note that in all four seasons there is a small occurrence of echoes in a narrow region around 100 km between 17:00 and 19:00 LT. In addition, note the occurrence of F-region irregularities between 20:00 and 22:00 LT (narrow vertical band covering all heights) during the spring and summer seasons.

In Fig. 9 we can see clearly a semidiurnal pattern, particularly in the lower heights. As height increases, the semidiurnal pattern starts to disappear during all seasons. Moreover,
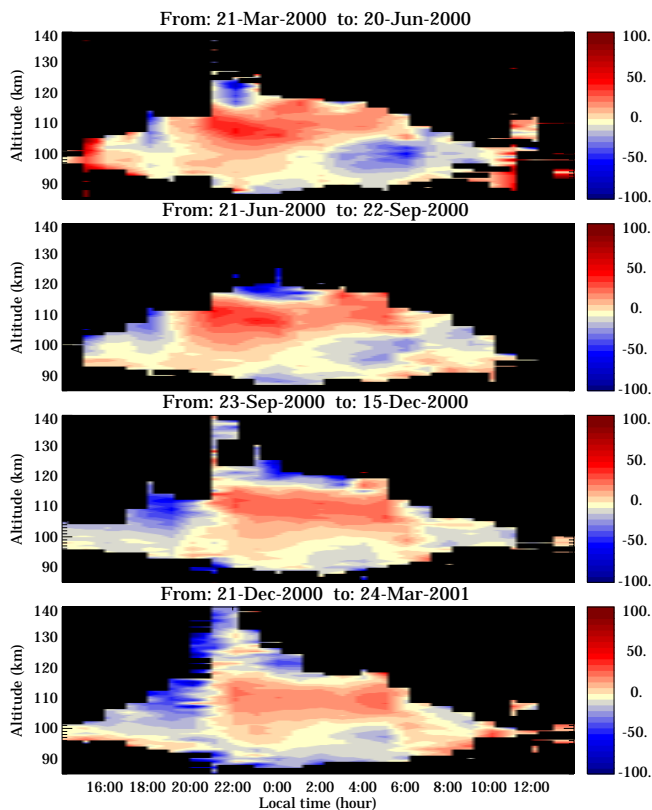
Fig. 9. Diurnal Doppler velocity from E-region echoes as a function of altitude for different periods of the year: fall, winter, spring, and summer in the first, second, third and fourth rows, respectively. No valid data are represented in black color.

after midnight we can see a wave in the vertical direction with an average wavelength of about 20 km. The amplitude of this wave behavior is larger during the fall and winter seasons.

3.2 Continuous F-region observations

As it was mentioned before, sometimes F-region irregularities are observed when experiments are set up to look at the E-region, since they come from higher altitudes and fall over the E-region sampling window (see Figs. 1 and 8). Knowing that the highest E-region echoes come from below 130 km, we have used the echoes above 130 km (SNR > 0 dB) as proxy measurements of the F-region irregularities. Although this is not a good way to obtain morphological characteristics of these echoes, we can still use this information to obtain their seasonal characteristics. From the 18 months of observations, we have seen (results not shown here) that "plume"-like F-region echoes occur only between September and April.

4 Discussion

In this section, we first discuss the E-region results obtained with the new continuous data set, putting special emphasis on seasonal and diurnal occurrences and the characteristics of the mean Doppler velocities. Then, we will discuss the relationship between E- and F-region irregularities, including the Jicamarca F-region measurements.

Before we continue, it is important to mention that the continuous data set may be slightly contaminated by meteor echoes, given the poor time resolution and the sampling window used. Apparently, there is a possible connection between the occurrence of the Piura E-region FAI and meteors, since most of the meteor echoes come from the north beam (i.e. from close to perpendicular to B). Nonetheless, we do not expect that the meteor echoes contaminate much of our results, taking into account that their occurrence rate over Piura is small (S. Avery, personal communication); therefore, the probability of obtaining meteor echoes when we receive E-region echoes is low.

4.1 E-region: Diurnal and seasonal occurrences

Our results confirm that the Piura E-region irregularities occur mainly at night. Moreover, they occur all year long. The maximum occurrence that is accompanied by the maximum SNR is observed during the local summer months, while the minimum occurrence (and minimum SNR) happens between April and June. In the Introduction, we have mentioned that the low latitude E-region FAI resemble more the mid-latitude echoes than those from the EEJ, i.e. they are generated mainly by the gradient drift instability rather than the two-stream instability and occur mainly at night. However, the mid-latitudes echoes are considered only a summertime phenomena (e.g. Tanaka and Venkateswaran, 1982; Haldoupis and Schlegel, 1996).

Now we compare the Piura diurnal and seasonal characteristics, to those obtained during the IGY with a CW VHF forward-scatter experiment at a similar dip latitude ($\sim$5° N), especially with a radar link between Huancayo (Peru) and Guayaquil (Ecuador). These observations were made during solar max conditions (the continuous observations were also obtained under solar max conditions), and the Bragg wavelength was $\sim$24 m (3 m for Piura). Moreover, there was no altitude discrimination from these forward-scatter observations, so the results obtained represent integrated values along all the E-region scattering heights. The specific details of the experiment and results can be found in Cohen and Bowles (1963).

The main features of this forward scatter experiment that are similar to the Piura echoes are (see Cohen and Bowles, 1963, Fig. 19):

– Nighttime echoes were observed all year long.

– The nighttime echoes were stronger around summer months, and weaker during winter months.

– The daytime echoes occur more frequently between March and September than during the other months. Nonetheless, these signals were much weaker than those observed in the EEJ region.

– The strongest daytime echoes were observed between 16:00 LT and 18:00 LT between October and January.

Although, the daytime signals at 5° N were weaker than in the EEJ, in general the daytime and nighttime echoes at this latitude were of comparable magnitude. Recall that at Piura, the nighttime echoes are much stronger than the daytime echoes. We believe this difference is because the 5° N forward-scatter echoes are closer to the EEJ region than the Piura echoes, and, therefore, subject to the EEJ influence. Although statistically, the EEJ region is known to cover ±3° from the dip equator, we know this boundary is not fixed. Moreover, Cohen and Bowles (1963) found that there is a strong asymmetry between radar echoes observed at 5° N and 5° S, with the southern echoes stronger (during the day and night) than the northern echoes. We believe the southern echoes present more similarities to the EEJ echoes. This result is still puzzling and needs further investigation.

In the Indian sector, using the Gadanki MST radar, daytime echoes have been frequently observed. Nonetheless, these echoes were weaker than the nighttime echoes and were confined to the very low altitudes (e.g. Krishna Murthy et al., 1998). Given that the Piura and Gadanki radars are located almost at the same dip latitude and assuming that there is not much longitudinal dependence on the occurrence of these echoes, daytime echoes are not observed much at Piura because of lower sensitivity (smaller antenna and less transmitted power). As in the case of mid-latitudes (e.g. Haldoupis and Schlegel, 1996), the "absence" of daytime echoes is probably due to the smoothing of electron density gradients due to strong solar photoionization production, and electric field shortening effects due to conductivity enhancements, causing the gradient drift instability to be inefficient during the day.

At this point we are still not in a position to determine the origin of the observed diurnal and seasonal characteristics, given the limited radar observations and the lack of knowledge of other important variables at these latitudes (e.g. density gradients, electric fields, etc.) However, knowing the close similarities with mid-latitudes echoes and with the present knowledge, these echoes might come from the combined action of more than one agent, e.g. sporadic E (E_s) layer, ambient density gradient and electric fields, neutral winds, etc.

For the mid-latitude case, Haldoupis and Schlegel (1996) found that the morphology (seasonal and diurnal behavior) of their echoes fits very much the well-known morphology of strong E_s layers. However, this does not mean necessarily that when E_s is present, backscatter echoes are always produced. In addition, sufficient large density gradients perpendicular to $\boldsymbol{B}$ and threshold electric fields parallel to those gradients could also be required for the instability to set in and operate.

Recently, Tsunoda et al. (1998) and Voiculescu et al. (1999) suggested the role of atmospheric planetary waves on the day-to-day variability of mid-latitude scatter echoes and strong E_s layers. Tsunoda et al. (1998) reported clear 5-day

periods on the midaltitude irregularities, while Voiculescu et al. (1999) found that the most commonly observed periods appear in two preferential bands, i.e. the 2 to 3 day and the 4 to 6 day band. We believe that planetary waves are also responsible for the day-to-day variability of the Piura E-region echoes (see Figs. 4 and 5). However, a detailed study on this variability will be left for future work.

4.2 E-region: mean Doppler velocities

Before we continue, one should keep in mind that the radar is sensitive to plasma waves propagating perpendicular to the Earth's magnetic field and that the Doppler shifts are due to the phase velocities of the scattering waves. Then, the Doppler velocities are interpreted as the line-of-sight projection of the $\boldsymbol{E} \times \boldsymbol{B}$ electron drift speeds, Doppler shifted by the neutral winds. At Piura, the magnetic declination is close to zero (1.28°), and since the radar points 14° to the north to become perpendicular to $\boldsymbol{B}$, we will consider the zonal (i.e. east-west) influences negligible. Thus, the observed Doppler velocity can be represented as:

$$V_r \propto - \left[\frac{\boldsymbol{E} \times \boldsymbol{B}_{\text{drifts}}}{1 + \psi} + \frac{\psi}{1 + \psi} v \cos \theta \right], \tag{1}$$

where ψ is the anisotropy factor defined by $\psi = \nu_e \nu_i / \Omega_e \Omega_i$. The ν_j and Ω_j terms refer to the ion-neutral collision frequencies and cyclotron frequencies, respectively, for species j, v is the meridional wind component and θ is the elevation pointing angle ($\sim$76°). We are neglecting the contributions of vertical neutral winds.

Given that the E-region altitudes are linked to the lower F-region over the dip equator, and that within a few degrees of the dip equator the vertical plasma motions result essentially from electrodynamic drifts driven by the zonal electric fields (Fejer, 1997), we consider that the Piura E-region drifts are mainly influenced by the equatorial F-region drifts. From (1), if $\psi \ll 1$ ($\psi \gg 1$), the Doppler velocities represent the $\boldsymbol{E} \times \boldsymbol{B}$ "vertical" equatorial F-region drifts (projected meridional winds), given that the ψ is the dominant factor.

In the lower E-region (below 100 km) $\psi \geq 1$ (Fejer et al., 1975), thus Doppler velocities at these heights represent the meridional winds. Therefore, it is not surprising to see that echoes from this region are of a continuous type. Moreover, as it was observed by Urbina et al. (2000), echoes from this lower region may be due to volume scattering.

As altitude increases, ψ decreases and the $\boldsymbol{E} \times \boldsymbol{B}$ contribution starts to dominate. This fact explains the predominant positive Doppler velocities in the upper region, which is consistent with the downward nighttime F-region vertical drifts measured at Jicamarca. Since the nighttime downward drifts over Jicamarca have large seasonal and solar cycle variations (e.g. Fejer, 1991), a detailed study is needed to arrive at better conclusions, for example, making concurrent comparisons for different seasons and solar flux conditions.

Under these considerations, our results suggest that: (1) there is a consistent, semidiurnal wave in the meridional wind during all seasons with a southward (northward) phase

before (after) midnight; (2) when the amplitude of the semidiurnal wave becomes larger, i.e. between April and June, the E-region echoes becomes weaker and occur less frequently; (3) northward winds are, on average, larger than the southward winds, and could be as large as $100 - 150 \, \mathrm{m \, s^{-1}}$, particularly between the April and June months; (4) although we observe a vertical wave in the Doppler velocity, it is difficult to interpret it without having an independent concurrent measurement of either the $\boldsymbol{E} \times \boldsymbol{B}$ drifts or the meridional winds.

At mid-latitudes using the Clemson HF radar, Hysell and Burcham (1999) also observed a correlation between the strength of the echoes and the direction of the Doppler velocities, namely the strongest echoes seemed generally to turn on and intensify when the Doppler velocities were away from (upward/northward) the radar and to diminish when the Doppler velocities were towards (downward/southward) the radar. Recently, Schlegel and Gurevich (1997) proposed a possible dependence of the backscatter echo intensity on neutral turbulence (as well as ionospheric parameters), particularly for lower E-region irregularities. Although our results suggest that the meridional winds can influence the growth rate of the irregularities, the way they do it is beyond the scope of the current paper.

Performing a harmonic analysis to the Gadanki lower E-region Doppler velocities, Krishna Murthy et al. (1998) also found a semidiurnal component in their data, along with a diurnal component. Their results are based on a few days taken in September 1994, and they found that the peak amplitude of the southward phase of their semidiurnal wave was around 00:00 LT, with an average amplitude of $10 \, \mathrm{m \, s^{-1}}$. These results are not in agreement with ours, however, one has to consider that the Gadanki radar is in the northern geographic hemisphere, at almost opposite longitude and based only on a few days of data.

4.3 E- vs. F-region irregularities

Although we have not obtained good morphological characteristics of the F-region irregularities over Piura, the weak Piura F-region echoes obtained suggest that they are very similar to those observed at the dip equator, contrary to the E-region irregularities that resemble more the mid-latitude echoes mainly because (1) there is a one-to-one correlation between the occurrence of Piura F-region echoes and the occurrence of topside ESF echoes (as observed from Jicamarca); and (2) their seasonal occurrence is similar to the seasonal occurrence of topside ESF at Jicamarca (e.g. Hysell and Burcham, 1998). In addition, our conclusion is also supported by the Gadanki observations (e.g. Patra et al., 1997). In the future, we are planning to improve the Piura radar sensitivity (wider pulse width and more transmitted averaged power), to obtain better echoes from these irregularities. Maybe with more sensitivity, it would be possible to see signatures at Piura of the bottomside/bottomtype layers seen at Jicamarca. Moreover, our results suggest that the likelihood of obtaining F-region irregularities over Piura,

and, therefore, topside ESF irregularities over Jicamarca, is greater ($\sim$0.5) when there are no E-region irregularities over Piura than when they are present ($\sim$0.2). Nonetheless, in our current analysis, we have considered events taken at different seasons; therefore, a more careful analysis will be done in the future to separate events when F-region irregularities are not expected, i.e. between May and August. On the other hand, there is more probability of observing bottom-type/bottomside ESF irregularities over Jicamarca when E-region irregularities are observed over Piura. The latter result is understandable given that the Piura E-region heights ($90 - 120 \, \mathrm{km}$) map to the very low F-region heights over Jicamarca (i.e. $190 - 220 \, \mathrm{km}$). Nonetheless, from our current results, there is not a straightforward relationship that could help us with the understanding of the ESF seeding mechanism.

5 Conclusions

In general, we have been able to corroborate most of the characteristics of the E-region irregularities already published by Woodman et al. (1999) using only a few days of data, namely that the Piura E-region echoes (1) occur mainly at night, (2) are generated by the gradient drift instability, and (3) could be classified into lower and upper region echoes. Based on 18 months of continuous observations, the seasonal and diurnal occurrences, as well as Doppler velocities, have also been presented and discussed. The morphological characteristics of the lower echoes and their Doppler velocities suggest that these echoes are strongly influenced by neutral winds and may be due to volume scattering. We will verify this assertion and study in detail the morphology of the quasi-periodic echoes by adding interferometry capabilities to the Piura system. The upper echoes are very structured in height and time. For example, on some occasions, we have observed the coexistence of positive and negative quasi-periodic striations (Chau et al., 2000). We expect to perform imaging studies of these irregularities similar those performed at Jicamarca (Hysell and Chau, 2002), to obtain a better understanding of the temporal (less than 1 min) and spatial (inside the illuminated volume) characteristics of the E-region echoes.

As it has been suggested by Krishna Murthy et al. (1998), we also attribute the Doppler velocity (downward/southward) of the upper E-region echoes to be mainly influenced by the equatorial F-region vertical drifts. On the other hand, the Doppler velocities of the lower E-region echoes represent mainly the meridional winds. Therefore, these radar measurements could provide nighttime meridional winds at these equatorial altitudes that are poorly measured. Moreover, if simultaneous experiments are performed with the Jicamarca incoherent scatter radar in order to obtain profiles of vertical drifts and reasonable models are used to obtain good values of the anisotropy factor, it could be possible to infer the meridional winds at all altitudes where the Piura E-region irregularities occur, i.e. between 90 and 120 km.

Finally, our observations of F-region irregularities over Piura suggest that (1) the Piura F-region echoes are well correlated with topside ESF irregularities over Jicamarca, (2) the likelihood of obtaining F-region irregularities over Piura, and, therefore, topside ESF over Jicamarca, is greater when E-region irregularities are not observed; and (3) there is more probability of observing bottomtype/bottomside ESF irregularities over Jicamarca when E-region irregularities are observed over Piura.

References

Chau, J. L. and Woodman, R. F.: Low-latitude quasiperiodic echoes observed with the Piura VHF radar in the E-region, Geophys. Res. Lett., 26, 2167–2170, 1999.

Chau, J. L., Woodman, R. F., and Flores, L. A.: Observations of E-region field-aligned irregularities just outside the equatorial electrojet region, paper presented at X International Symposium on Equatorial Aeronomy, Antalya, Turkey, May 17-23, 2000.

Choudhary, R. K. and Mahajan, K. K.: Tropical E-region field aligned irregularities: Simulatneous observations of continuous and quasiperiodic echoes, J. Geophys. Res., 104, 2613–2619, 1999.

Choudhary, R. K., Mahajan, K. K., Singh, S., Kumar, K., and Anandan, V. K.: First VHF radar observations of tropical latitude E-region field aligned irregularities, Geophys. Res. Lett., 23, 3683–3686, 1996.

Cohen, R. and Bowles, K. L.: Ionospheric VHF scattering near the magnetic equator during the International Geophysical Year, J. Res. Natl. Bur. Stand. U. S., Sect. D, 67, 459–480, 1963.

Fejer, B. G.: Low latitude electrodynamic plasma drifts: A review, J. Atmos. Sol. Terr. Phys., 43, 377–386, 1991.

Fejer, B. G.: The electrodynamics of the low-latitude ionosphere: Recent results and future challenges, J. Atmos. Sol. Terr. Phys., 59, 1465–1482, 1997.

Fejer, B. G. and Kelley, M. C.: Ionospheric irregularities, Rev. Geophys. Space Phys., 18, 401–454, 1980.

Fejer, B. G., Farley, D. T., Balsley, B. B., and Woodman, R. F.: Vertical structure of the VHF backscattering region in the equatorial electrojet and the gradient drift instability, J. Geophys. Res., 80, 1313–1324, 1975.

Forbush, S. E. and Casaverde, M.: Equatorial electrojet in Peru, Carnegie Inst. Washington Publ., 620, 1–37, 1961.

Fukao, S., Kelley, M. C., Shirakawa, T., Takami, T., Yamamoto, M., Tsuda, T., and Kato, S.: Turbulen upwelling of the mid-latitude ionosphere 1. Observational results by the MU radar, J. Geophys. Res., 96, 3725–3746, 1991.

Fukao, S., Yamamoto, M., Tsunoda, R. T., Hayakawa, H., and Mukai, T.: The SEEK (Sporadic-E experiment over Kyushu) campaign, Geophys. Res. Lett., 25, 1761–1764, 1998.

Gage, K. S., Balsley, B. B., Ecklund, W. L., Carter, D. A., and McAfee, J. R.: Wind profiler-related research in the tropical Pacific, J. Geophys. Res., 96, 3209–3220, 1991.

Haldoupis, C. and Schlegel, K.: Characteristics of midlatitude cherent backscatter from ionospheric E region obtained with sporadic E scatter experiment, J. Geophys. Res., 101, 13 387–13 397, 1996.

Hysell, D. L. and Burcham, J. D.: JULIA radar studies of equatorial spread f, J. Geophys. Res., 103, 29 155–29 167, 1998.

Hysell, D. L. and Burcham, J. D.: HF radar observations of quasiperiodic E layer echoes over North America, J. Geophys. Res., 104, 4361–4371, 1999.

Hysell, D. L. and Burcham, J. D.: The 30-MHz radar interferometer studies of midlatitude E region irregularities, J. Geophys. Res., 105, 12 797–12 812, 2000.

Hysell, D. L. and Chau, J. L.: Imaging radar observations and non-local theory of large-scale waves in the equatorial electrojet, Ann. Geophysicae, this issue, 20, 1167–1179, 2002.

Kelley, M. C.: The Earth's Ionosphere: Plasma Physics and Electrodynamics, Academic, San Diego, Calif., 1989.

Krishna Murthy, B. V., Ravindran, S., Viswanathan, K. S., Subbarao, K. S. V., Patra, A. K., and Rao, P. B.: Small-scale (∼3 m) E-region irregularities at and off the magnetic equator, J. Geophys. Res., 103, 20 761–20 772, 1998.

Larsen, M. F.: Coqui 2: Mesospheric and lower thermospheric wind observations over Puerto Rico, Geophys. Res. Lett., 27, 445–448, 2000.

Patra, A. K. and Rao, P. B.: High-resolution radar measurements of turbulent structure in the low-latitude E-region, J. Geophys. Res., 104, 24 667–24 673, 1999.

Patra, A. K., Rao, P. B., Anandan, V. K., and Jain, A. R.: Radar observations of 2.8 m equatorial spread-F irregularities, J. Atmos. Sol. Terr. Phys., 59, 1633–1641, 1997.

Rao, P. B., Patra, A. K., Sarma, T. V. C., Murthy, B. V. K., Rao, K. S. V. S., and Hari, S. S.: Radar observations of updrafting and downdrafting plasma depletions associated with the equatorial spread F, Radio Sci., 1215-1227, 32, 1997.

Schlegel, K. and Gurevich, A. V.: Radar backscatter from plasma irregularities of the lower E-region induced by neutral turbulence, Ann. Geophysicae, 15, 870–877, 1997.

Swartz, W. E., Kelley, M. C., Makela, J. J., Collins, S. C., Kudeki, E., Franke, S., Urbina, J., Aponte, N., Sulzer, M. P., and Gonzalez, S. A.: Coherent and incoherent scatter radar observations during intense mid-latitude spread F, Geophys. Res. Lett., 27, 2829–2832, 2000.

Tanaka, T. and Venkateswaran, S. V., Characteristics of field-aligned E-region irregularities over Iioka (36° N), Japan, J. Atmos. Sol. Terr. Phys., 44, 381–393, 1982.

Tsunoda, R. T., Yamamoto, M., Igarashi, K., Hocke, L., and Fukao, S.: Quasi-periodic radar echoes from midlatitude sporadic-E and role of the 5-day planetary wave, Geophys. Res. Lett., 25, 951–954, 1998.

Urbina, J., Kudeki, E., Franke, S. J., Gonzalez, S., Zhou, Q., and Collins, S. C.: 50 MHz radar observations of mid-latitude E-region irregularities at Camp Santiago, Puerto Rico, Geophys. Res. Lett., 27, 2853–2856, 2000.

Voiculescu, M., Haldoupis, C., and Schlegel, K.: Evidence fro planetary wave effects on midlatitude backscatter and sporadic E-layer occurrence, Geophys. Res. Lett., 26, 1105–1108, 1999.

Woodman, R. F. and La Hoz, C.: Radar observations of F-region equatorial irregularities, J. Geophys. Res., 81, 5447–5466, 1976.

Woodman, R. F., Chau, J. L., Aquino, F., Rodriguez, R. R., and Flores, L. A.: Low-latitude field-aligned irregularities observed in the E-region with the Piura VHF radar: First results, Radio Sci., 34, 983–990, 1999.

Yamamoto, M., Fukao, S., Woodman, R. F., Ogawa, T., Tsuda, T., and Kato, S.: Midlatitude E-region field-aligned irregularities observed with the MU radar, J. Geophys. Res., 96, 15 943–15 949, 1991.

Yamamoto, M., Fukao, S., Ogawa, T., and Tsuda, T.: A morphological study on mid-latitude E-region field-aligned irregularities observed with the MU radar, J. Atmos. Sol. Terr. Phys., 54, 769–777, 1992.